

## Supporting Information

	Experimental section	S2
	Materials and instruments	
	Synthetic procedures	S3
	Characterization data for compound <b>1</b> .	S4
<b>Figure S1</b>	AT IR spectrum of <b>1</b> .	S3
<b>Figure S2</b>	NMR analysis of <b>1</b> in DMSO- $d_6$ , a) $^1H$ , and b) $^{13}C$ .	S4
<b>Figure S3</b>	Experimental (Up) and theoretical (down) ISOTOPIC pattern for the $[M-Br]^+$ ion of compound <b>1</b> (mass error: -0.2 ppm)	S5
	Characterization data for compound <b>2</b> .	S6
<b>Figure S4</b>	AT IR spectrum of <b>2</b> .	S7
<b>Figure S5</b>	NMR analysis of <b>2</b> in $CDCl_3$ , a) $^1H$ , b) $^{13}C$ , c) $\{^1H, ^1H\}$ COS90, and d) $\{^{13}C, ^1H\}$ HSQC.	S7
<b>Figure S6</b>	Experimental (Up) and theoretical (down) ISOTOPIC pattern for the $[M-Br]^+$ ion of compound <b>2</b> (mass error: -0.4 ppm)	S10
	Characterization data for compound <b>3</b> .	S11
<b>Figure S7</b>	AT IR spectrum of <b>3</b> .	S12
<b>Figure S8</b>	NMR analysis of <b>3</b> in DMSO- $d_6$ , a) $^1H$ , b) $^{13}C$ , c) $^{19}F$ d) $\{^1H, ^1H\}$ COS90 and e) $\{^{13}C, ^1H\}$ HSQC.	S12
<b>Figure S9</b>	Experimental (Up) and theoretical (down) ISOTOPIC pattern for the a) $[M+K]^+$ (mass error: -0.6 ppm), b) $[M+Na]^+$ (mass error: -0.9 ppm) and c) $[M+H]^+$ ion (mass error: -0.5 ppm) of compound <b>3</b> .	S15
	Single-crystal X-ray diffraction analysis	S17
<b>Table S1</b>	Selected experimental bond lengths (Å) and angles (°) of <b>3</b> .	S18
<b>Figure S10</b>	Electronic absorption spectra of <b>3</b> in different solvents.	S19
<b>Figure S11</b>	Electronic absorption spectra of <b>1</b> in different solvents.	S19
<b>Figure S12</b>	Calculated electronic absorption spectra of <b>1</b> and <b>3</b> .	S19
	Density functional theory (DFT) calculations	S20
<b>Table S2</b>	Selected FMO of <b>1</b> calculated at B3LYP/LANL2DZ level of theory.	S21
<b>Table S3</b>	Computed excitation energies (eV), electronic transition configurations and oscillator strengths ( $f$ ) of compounds <b>1</b> and <b>3</b> (selected, $f > 0.001$ ) (Selected)	S22
<b>Figure S13</b>	UV-Vis spectra of a) <b>1</b> and b) <b>3</b> in 20% (v/v) DMSO/PBS (0.1 M) recorded as a function of time during the incubation for 72 h.	S23
	Cell viability	S24
	Lysozyme binding affinity	S25
<b>Figure S14</b>	Deconvoluted ESI-MS spectra of HEWL treated with compound <b>1</b> in a) 1:10 and b) 1:20 (HEWL: complex).	S26
<b>Figure S15</b>	a) ESI MS spectrum of <b>3</b> . b) Deconvoluted ESI-MS spectrum of HEWL treated with compound <b>3</b> in 1:20 (HEWL: complex).	S27
	References	S28

## Experimental section

### Materials and instruments

Synthesis of tricarbonyl Re(I) compounds **1–3** was executed in oven-dried glassware under pure argon atmosphere, while the Schlenk vessels were protected from light by packaging with aluminum foil. Bromo pentacarbonyl rhenium(I) was supplied by Strem. 4,4,4-trifluoro-2-butynoic acid ethyl ester<sup>1</sup> and 4'-(2-pyridyl)-2,2':6',2''-terpyridine (terpy)<sup>2</sup> were prepared by the published methods. The other chemicals (e.g. solvents, sodium azide, etc...) were purchased from the commercial sources and used as received. Solid-state IR spectra were registered on a Nicolet 380 FT-IR spectrometer fitted with a smart iTR ATR accessory. Micro-elemental compositions (C, H, and N) of terpy and its Re(I) compounds were obtained experimentally by Elementar Vario MICRO cube CHN analyzer or an EA 3000 elemental analyser from HEKtech. Positive mode electrospray ionization mass spectra were recorded on ThermoFisher Exactive Plus instrument with an Orbitrap mass analyzer at a resolution of  $R = 70.000$  and a solvent flow rate of  $5 \mu\text{L min}^{-1}$ . The  $\{^1\text{H}, ^{13}\text{C}, \text{ and } ^{19}\text{F}\}$  NMR spectra were recorded with Bruker-Avance 500 ( $^1\text{H}$ , 500.13 MHz;  $^{13}\text{C}\{^1\text{H}\}$ , 125.77 MHz;  $^{19}\text{F}$ , 470.6 MHz) and Bruker-Avance 400 ( $^1\text{H}$ , 400.40 MHz;  $^{13}\text{C}\{^1\text{H}\}$ , 100.70 MHz) spectrometers. ( $\{^1\text{H}, ^1\text{H}\}$  COSY and  $\{^1\text{H}, ^{13}\text{C}\}$  HSQC) spectra were registered to precisely assign the resonances of the protons and carbons of the synthesized compounds.

## Synthetic procedures

### Synthesis of *fac*-[ReBr(CO)<sub>3</sub>(terpy-*k*<sup>2</sup>N<sup>1</sup>,N<sup>2</sup>)] (1)

0.36 mmol of the terpyridine ligand (112 mg) and [ReBr(CO)<sub>5</sub>] (0.44 mmol; 178 mg) were dissolved in degassed methanol (25 mL) under an atmosphere of pure argon and the reaction mixture was heated to reflux for 24 h in the dark. Orange precipitate was collected by filtration, washed with methanol, chloroform, diethyl ether and dried under vacuum. Yield: 82% (196 mg, 0.30 mmol). IR (ATR):  $\nu$  = 3082 (w, CH), 3052 (w, CH), 2011 (vs, C≡O), 1901 (vs, C≡O), 1873 (vs, C≡O), 1610 (m, CC/CN), 1470, 1400, 1305, 991, 780, 749 cm<sup>-1</sup>. <sup>1</sup>H NMR (400.40, DMSO-d<sub>6</sub>):  $\delta$  = 9.36 (s, 1H), 9.10 (m, 2H), 8.82 (m, 2H), 8.61 (d, <sup>3</sup>J<sub>H,H</sub> = 7.7 Hz, 1H), 8.53 (s, 1H), 8.39 (t, <sup>3</sup>J<sub>H,H</sub> = 8.8 Hz, 1H), 8.11 (td, <sup>3</sup>J<sub>H,H</sub> = 8.0 Hz, <sup>4</sup>J<sub>H,H</sub> = 1.6 Hz, 1H), 8.06 (td, <sup>3</sup>J<sub>H,H</sub> = 7.6 Hz, <sup>4</sup>J<sub>H,H</sub> = 1.5 Hz, 1H), 7.89 (d, <sup>3</sup>J<sub>H,H</sub> = 8.3 Hz, 1H), 7.80 (t, <sup>3</sup>J<sub>H,H</sub> = 6.0 Hz, 1H), 7.63 (m, 2H) ppm. <sup>13</sup>C NMR (100.68 MHz, DMSO-d<sub>6</sub>):  $\delta$  = 197.4 (C≡O), 193.9 (C≡O), 190.3 (C≡O), 161.7, 157.9, 157.5, 156.2, 152.9, 151.0, 150.3, 149.3, 149.0, 140.0, 137.9, 137.0, 127.5, 125.7, 125.4, 125.0, 124.9, 124.1, 122.7, 120.2 ppm. ESI-MS (positive mode, acetone):  $m/z$  = 581.0613 [M-Br]<sup>+</sup> (M: molecular mass). C<sub>23</sub>H<sub>14</sub>BrN<sub>4</sub>O<sub>3</sub>Re: C 41.82, H 2.14, N 8.48, found, C 41.74, H 2.31, N 8.49.

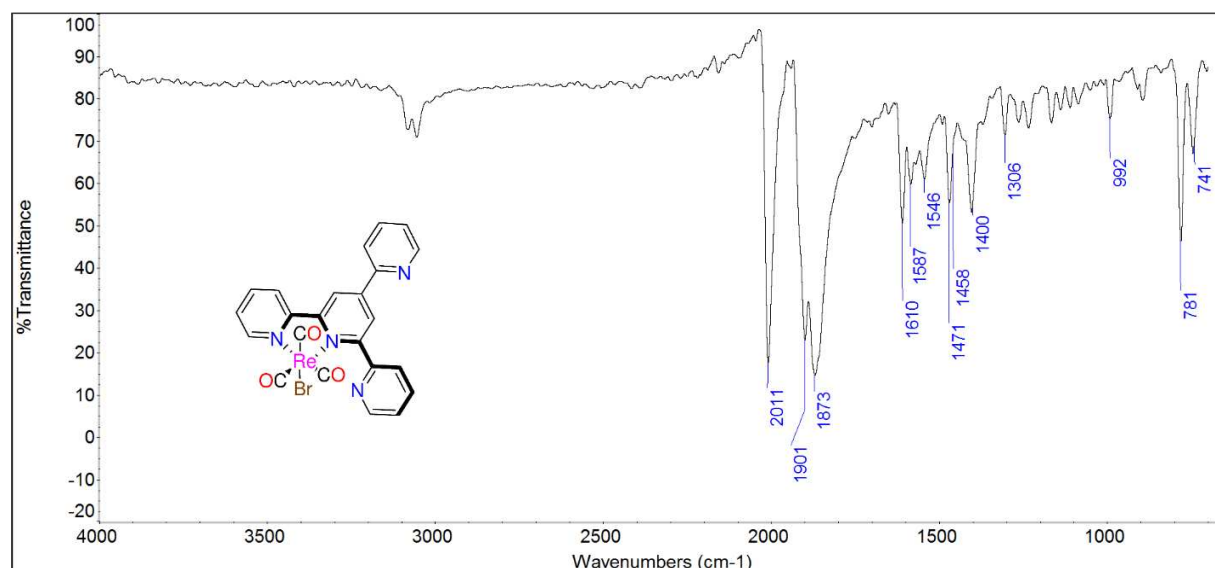
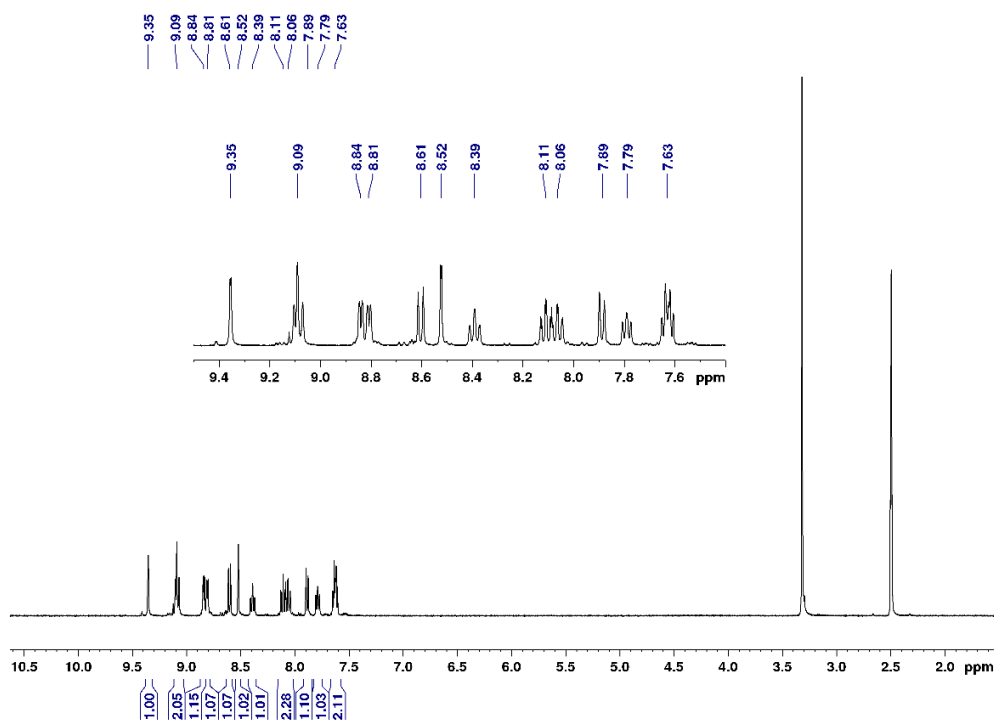
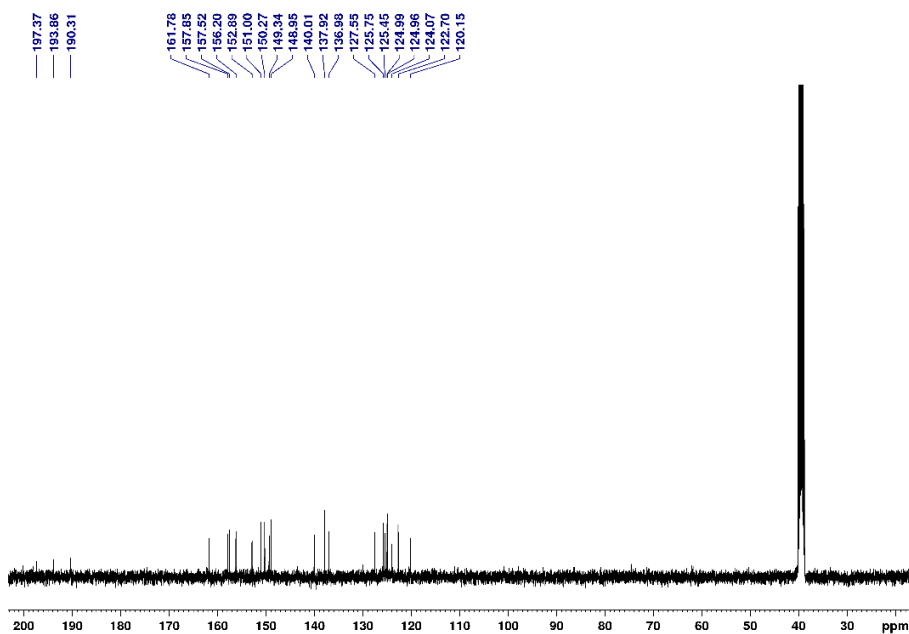


Figure S1 AT IR spectrum of 1.



a)



b)

Figure S2 NMR analysis of **1** in DMSO-d<sub>6</sub>, a) <sup>1</sup>H, and b) <sup>13</sup>C.

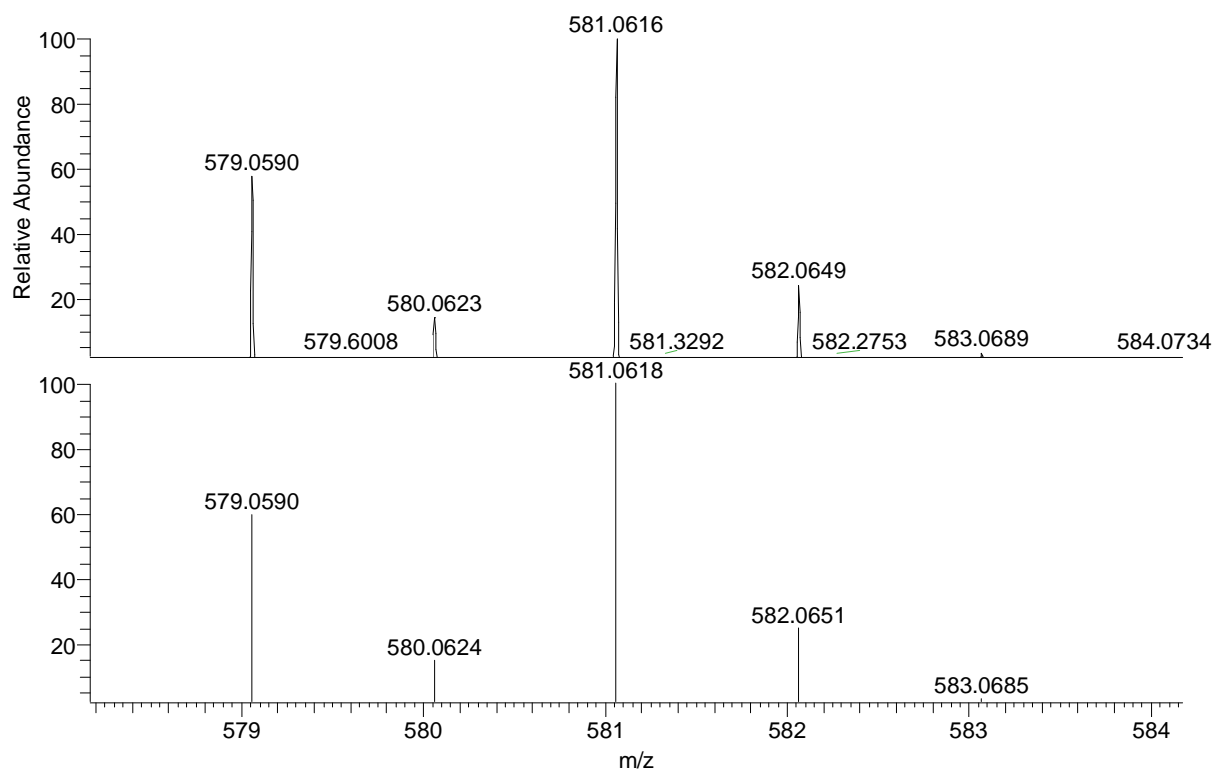


**Figure S3** Experimental (Up) and theoretical (down) ISOTOPIC pattern for [M-Br]<sup>+</sup> ion of compound **1** (mass error: -0.2 ppm)

## Synthesis of *fac*-[ReN<sub>3</sub>(CO)<sub>3</sub>(terpy-*k*<sup>2</sup>N',N'')] (2)

**Caution:** Azide metal-based compounds are exposed to sudden violent decomposition. Scratching of the azide compounds normally lead to explosion, and, hence, handling and purification with great care are vital.

To a flatted flask charged with **1** (150 mg, 0.23 mmol) and dichloromethane (25 mL), silver trifluormethane sulfonate (80 mg, 0.31 mmol) was added. The reaction mixture was stirred at the room temperature for 24 h, while the flask was protected from the light by packaging with aluminum foil. Silver bromide was filtered off through Celite. To the clear yellow solution was then added sodium azide (26 mg, 0.4 mmol) and stirring was continuing over a week. Small quantity of silver azide was carefully filtered off. Solvent was removed under pressure, and the resulting orange precipitate was washed with water (5 × 5 mL), diethyl ether (3 × 5 mL) and dried under vacuum. Yield: 78% (105 mg, 0.17 mmol). IR (ATR):  $\nu$  = 3090 (w, CH), 3052 (w, CH), 2055 (vs, N<sub>3</sub>), 2012 (vs, C≡O), 1930 (vs, C≡O), 1896 (vs, C≡O), 1614 (m, CC/CN), 1547, 1399, 781. <sup>1</sup>H NMR (500.13 MHz, CDCl<sub>3</sub>):  $\delta$  = 9.14 (m, 2H), 8.89 (d, <sup>3</sup>J<sub>H,H</sub> = 4.6 Hz, 1H), 8.85 (m, 1H), 8.51 (d, <sup>3</sup>J<sub>H,H</sub> = 8.0 Hz, 1H), 8.34 (s, 1H), 8.18 (t, <sup>3</sup>J<sub>H,H</sub> = 8.8 Hz, 1H), 8.05 (d, <sup>3</sup>J<sub>H,H</sub> = 8.0 Hz, 1H), 8.02 (t, <sup>3</sup>J<sub>H,H</sub> = 6.4 Hz, 1H), 7.94 (m, 2H), 7.61 (t, <sup>3</sup>J<sub>H,H</sub> = 6.2 Hz, 1H), 7.57 (t, <sup>3</sup>J<sub>H,H</sub> = 6.0 Hz, 1H), 7.5 (m, 1H) ppm. <sup>13</sup>C-NMR (125.75 MHz, CDCl<sub>3</sub>):  $\delta$  = 163.0, 157.7, 156.9, 153.1, 151.5, 150.6, 149.7, 149.3, 139.1, 137.6, 137.2, 126.9, 125.5, 125.4, 125.2, 124.9, 124.5, 124.2, 121.6, 120.0 ppm. ESI-MS (positive mode, acetone): *m/z* = 581.0616 [M-N<sub>3</sub>]<sup>+</sup>. C<sub>23</sub>H<sub>14</sub>N<sub>7</sub>O<sub>3</sub>Re: C 44.37, H 2.27, N 15.75, found, C 44.41, H 2.33, N 15.73.

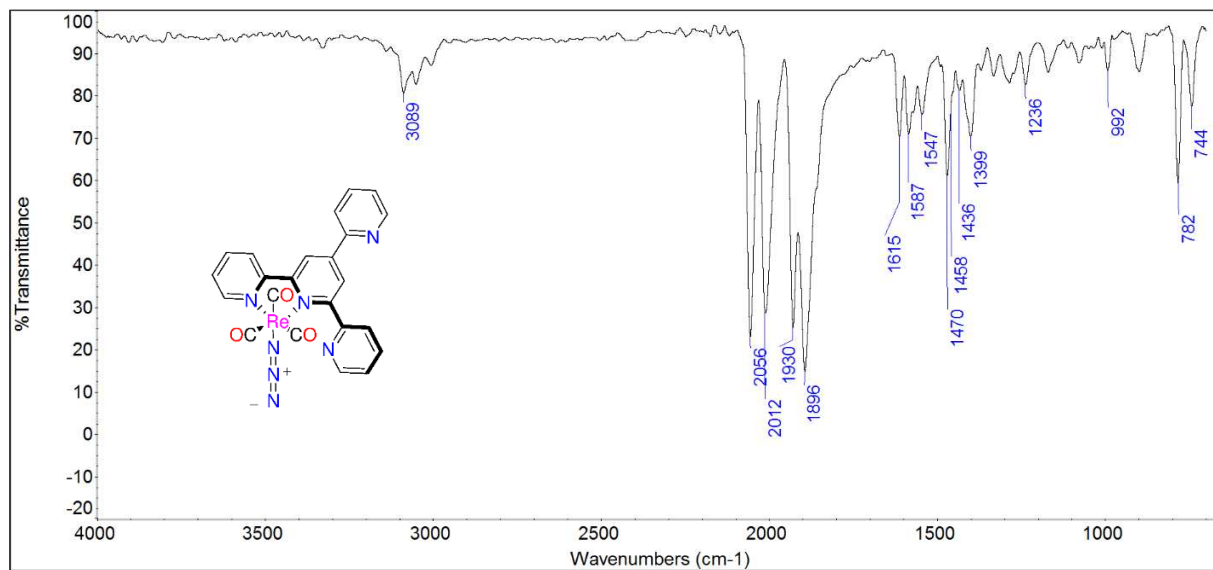
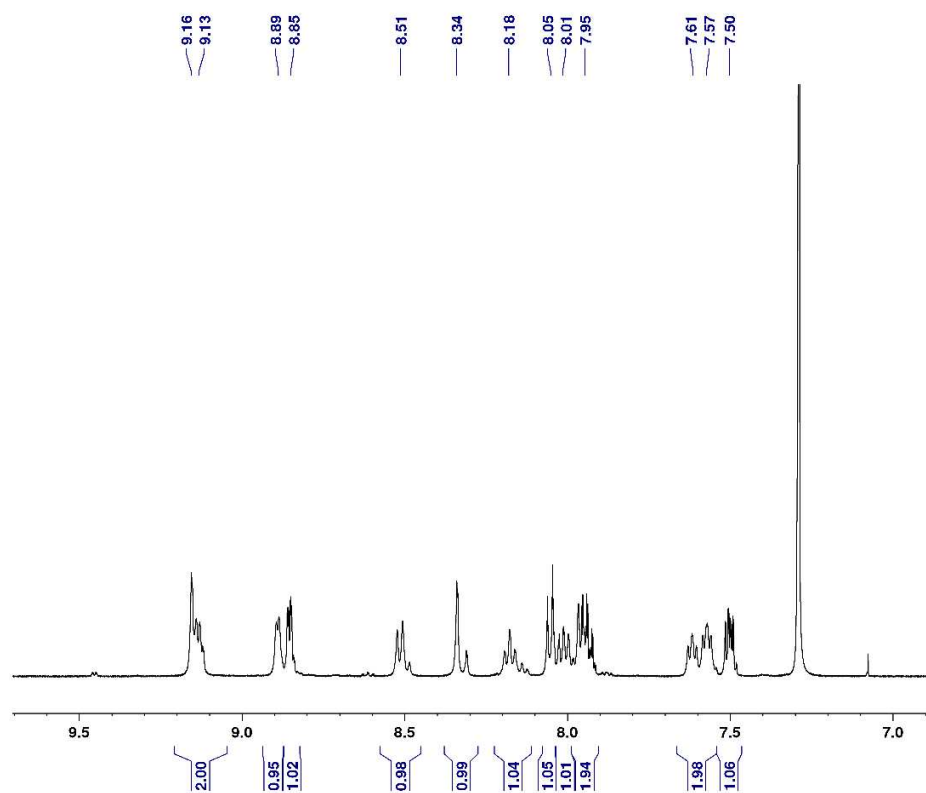
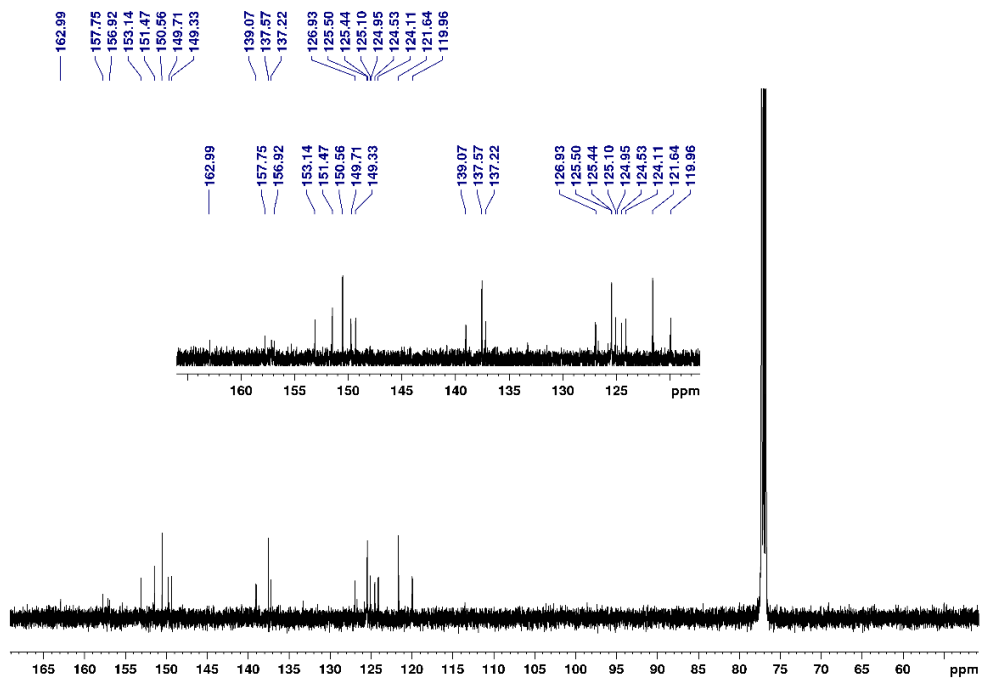
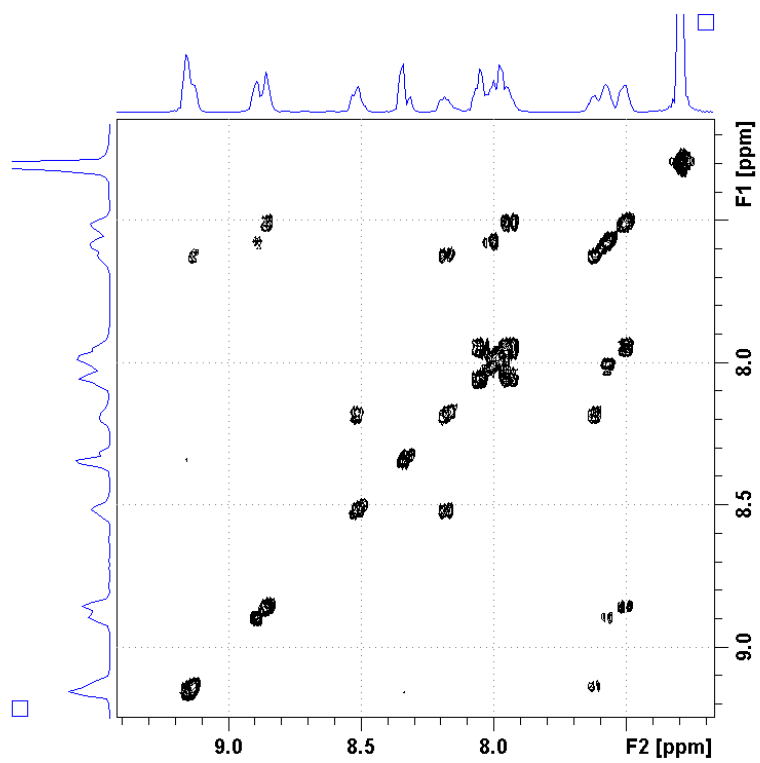


Figure S4 AT IR spectrum of 2.



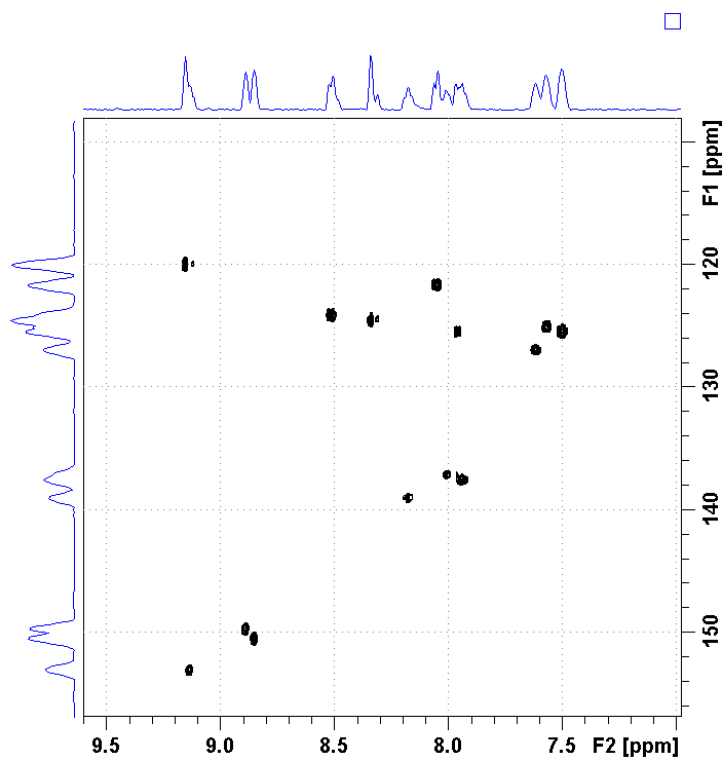


b)



c)

S8



d)

Figure S5 NMR analysis of **2** in  $\text{CDCl}_3$ , a)  $^1\text{H}$ , b)  $^{13}\text{C}$ , c)  $\{^1\text{H}, ^1\text{H}\}$  COSY, and d)  $\{^{13}\text{C}, ^1\text{H}\}$  HSQC.

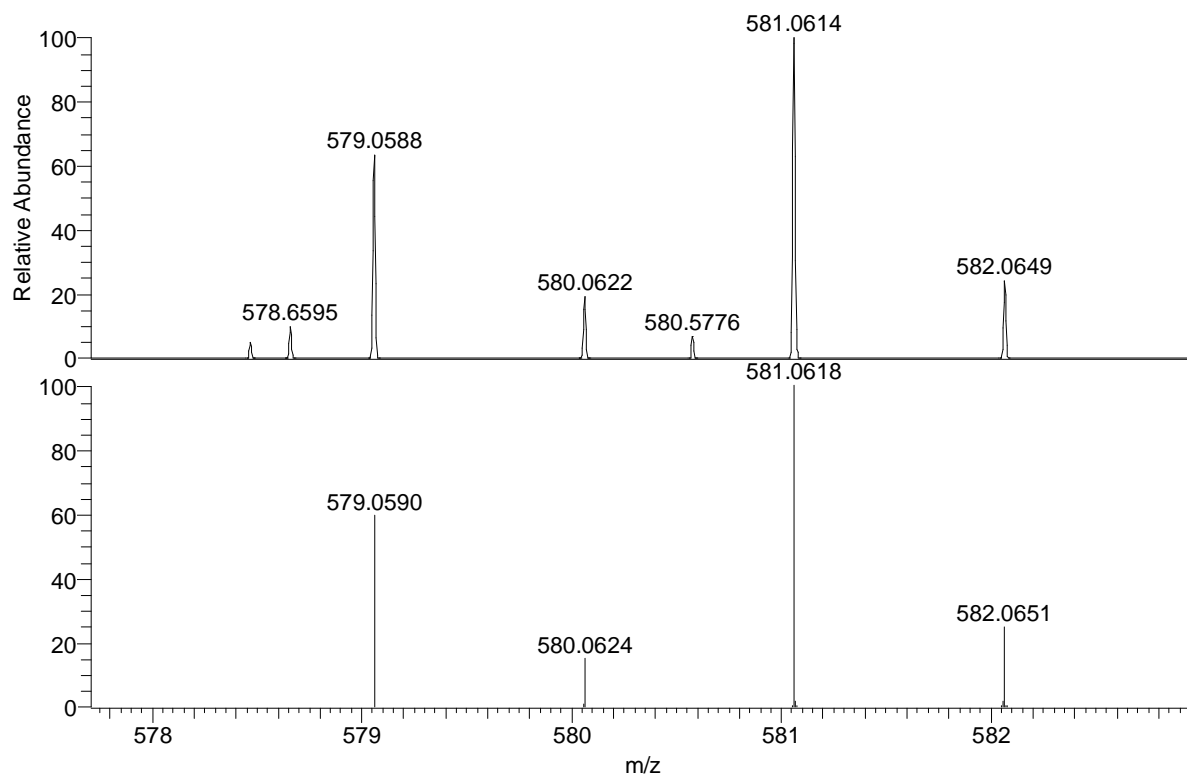


**Figure S6** Experimental (Up) and theoretical (down) ISOTOPIC pattern for the [M-Br]<sup>+</sup> ion of compound **2** (mass error: -0.4 ppm)

### Synthesis of *fac*-[Re(triazolate<sup>COOCH<sub>2</sub>CH<sub>3</sub>,CF<sub>3</sub></sup>)(CO)<sub>3</sub>(terpy-*k*<sup>2</sup>N<sup>1</sup>,N<sup>2</sup>)] (3)

4,4,4-trifluoro-2-butynoic acid ethyl ester (17 mg, 0.1 mmol) was added to the solution of **2** (60 mg, 0.096 mmol) in dichloromethane and then the reaction mixture was stirred at the room temperature for 7 d. Solvent was removed under pressure and the resulting orange precipitate was washed with hexane (3 × 5 mL), and dried under vacuum. Yield: 65% (58 mg, 0.082 mmol). IR (ATR):  $\nu = 2022$  (vs, C≡O), 1925 (vs, C≡O), 1899 (vs, C≡O), 1722 (s, C=O), 1619 (m, CC/CN), 1588, 1337, 1165, 1133, 1053, 783. <sup>1</sup>H NMR (500.13 MHz, CDCl<sub>3</sub>):  $\delta = 9.21$  (dd, <sup>3</sup>J<sub>H,H</sub> = 5.4 Hz, <sup>4</sup>J<sub>H,H</sub> = 0.9 Hz, 1H), 8.99 (d, <sup>4</sup>J<sub>H,H</sub> = 1.5 Hz, 1H), 8.85 (m, 1H), 8.82 (m, 1H), 8.40 (d, <sup>3</sup>J<sub>H,H</sub> = 8.3 Hz, 1H), 8.26 (d, <sup>4</sup>J<sub>H,H</sub> = 1.6 Hz, 1H), 8.16 (td, <sup>3</sup>J<sub>H,H</sub> = 7.7 Hz, <sup>4</sup>J<sub>H,H</sub> = 1.6 Hz, 1H), 8.01 (d, <sup>3</sup>J<sub>H,H</sub> = 8.0 Hz, 1H), 7.92 (m, 2H), 7.73 (d, <sup>3</sup>J<sub>H,H</sub> = 8.0 Hz, 1H), 7.55 (m, 2H), 7.48 (m, 1H), 4.21 (q, <sup>3</sup>J<sub>H,H</sub> = 7.3 Hz, 2H, CH<sub>2</sub>), 1.25 (t, <sup>3</sup>J<sub>H,H</sub> = 7.3 Hz, 3H, CH<sub>3</sub>) ppm. <sup>13</sup>C-NMR (125.75 MHz, CDCl<sub>3</sub>):  $\delta = 196.4$  (C≡O), 194.0 (C≡O), 193.1 (C≡O), 163.2 (C=O), 161.0, 158.1, 157.7, 157.3, 153.6, 151.5, 150.5, 149.5, 149.4, 139.1, 138.5 (q, <sup>2</sup>J<sub>C,F</sub> = 37.4 Hz, C–CF<sub>3</sub>), 137.6, 137.3, 136.5, 126.9, 125.4, 125.2, 125.1, 124.5, 123.7, 121.6, 121.4 (q, <sup>1</sup>J<sub>C,F</sub> = 268.2 Hz, –CF<sub>3</sub>), 119.7, 60.7 (CH<sub>2</sub>), 14.0 (CH<sub>3</sub>) ppm. <sup>19</sup>F NMR (470.6 MHz, CDCl<sub>3</sub>):  $\delta = -60.0$  (–CF<sub>3</sub>) ppm. ESI-MS (positive mode, acetone):  $m/z = 812.0842$  [M+Na]<sup>+</sup>, 790.1025 [M+H]<sup>+</sup>, 581.0616 [M–triazolate]<sup>+</sup>. C<sub>29</sub>H<sub>19</sub>F<sub>3</sub>N<sub>7</sub>O<sub>5</sub>Re: C 44.16, H 2.43, N 12.43, found, C 44.25, H 2.53, N 11.72. For synthetic organometallic compounds, the sensitivity of M–C, M–N, ....etc. bonds towards oxidation often complicates the elemental analysis data.<sup>3</sup> In addition, the elemental analyses of metal azide and triazolate compounds sometimes fall outside the acceptable error.<sup>4</sup> Therefore, the reported error (0.7%) in the nitrogen elemental analysis is expected.

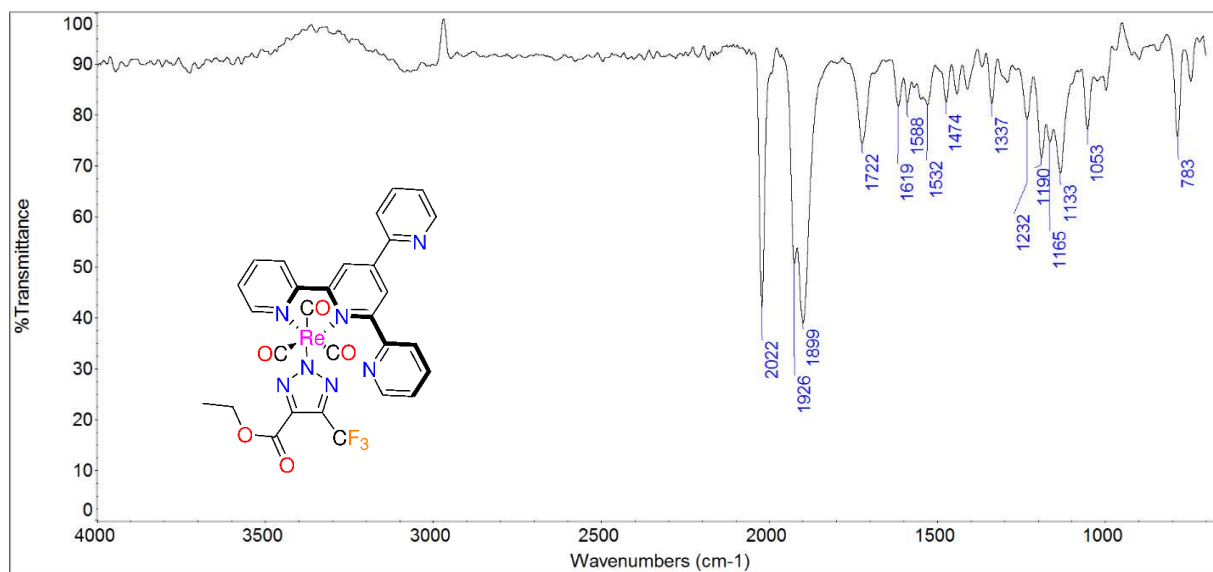
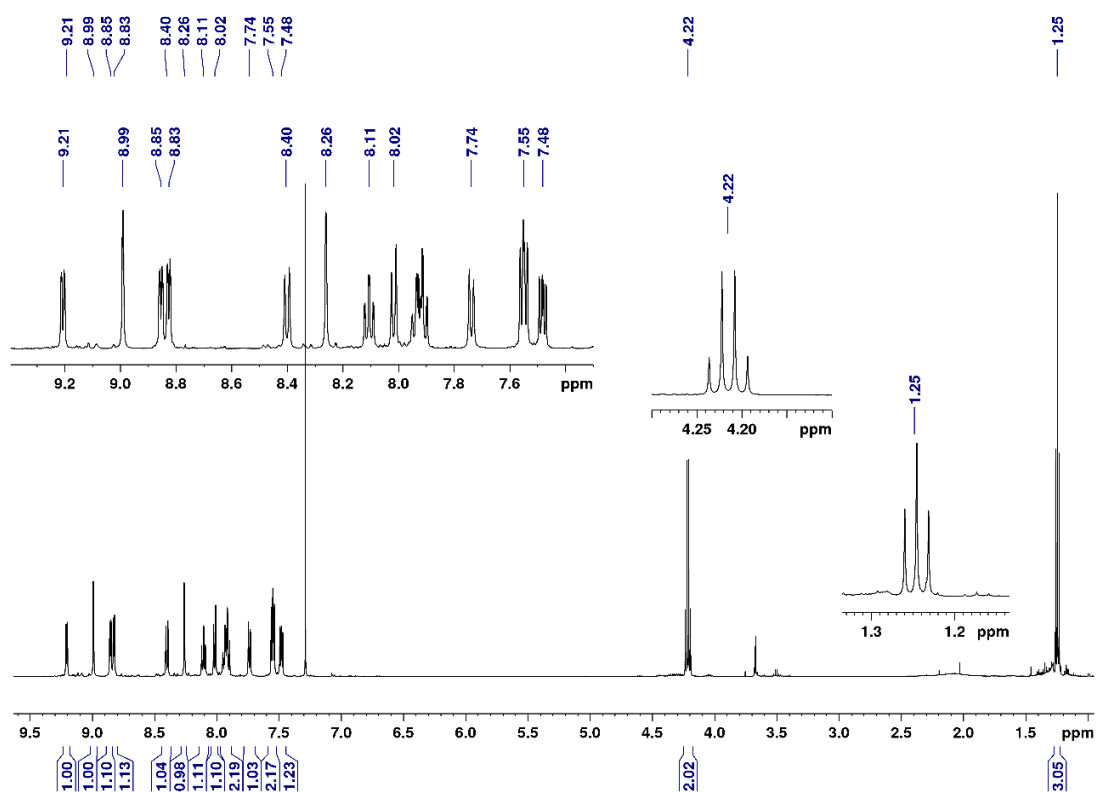
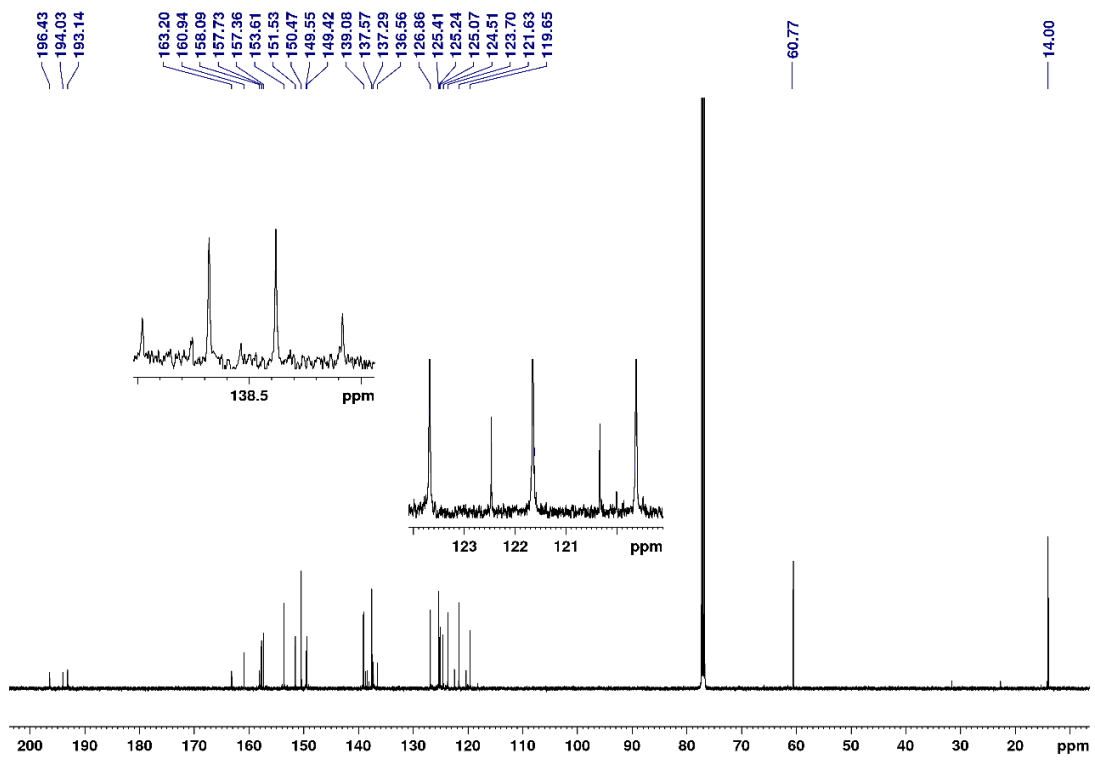


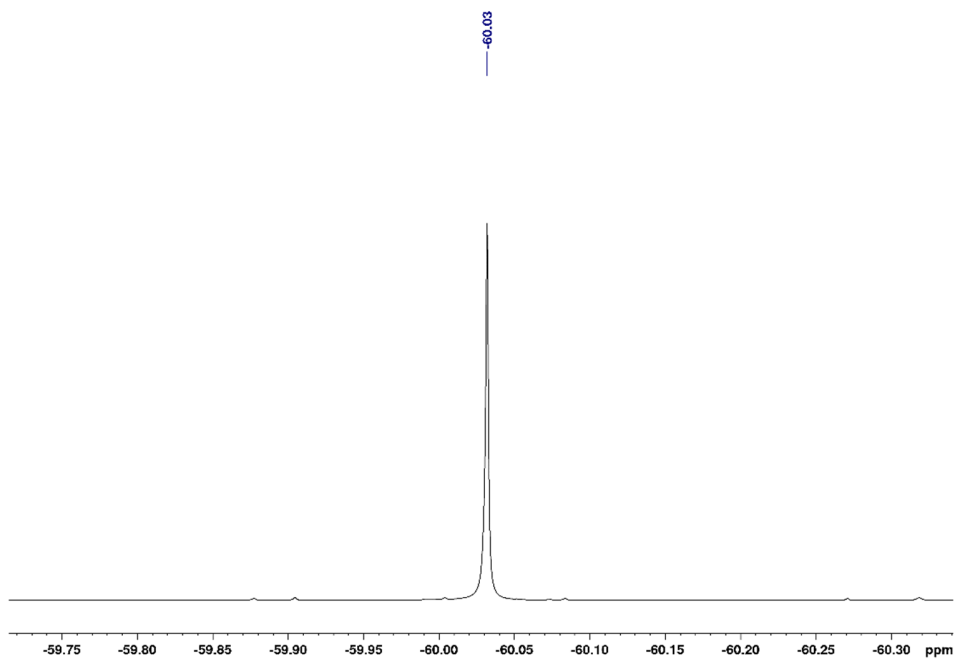
Figure S7 AT IR spectrum of **3**.



a)

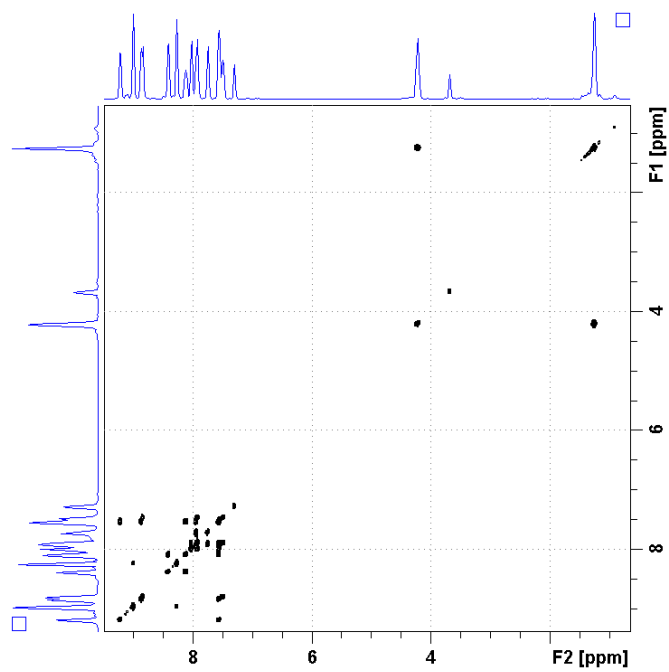


b)

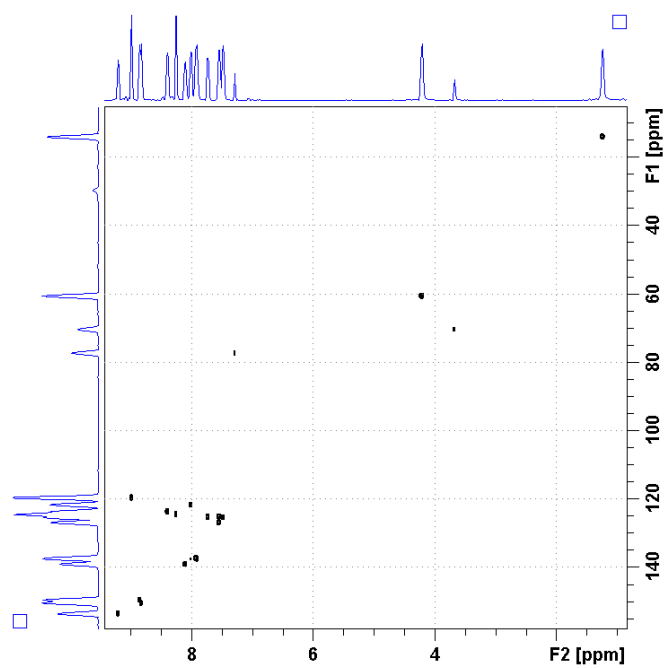


c)

S13

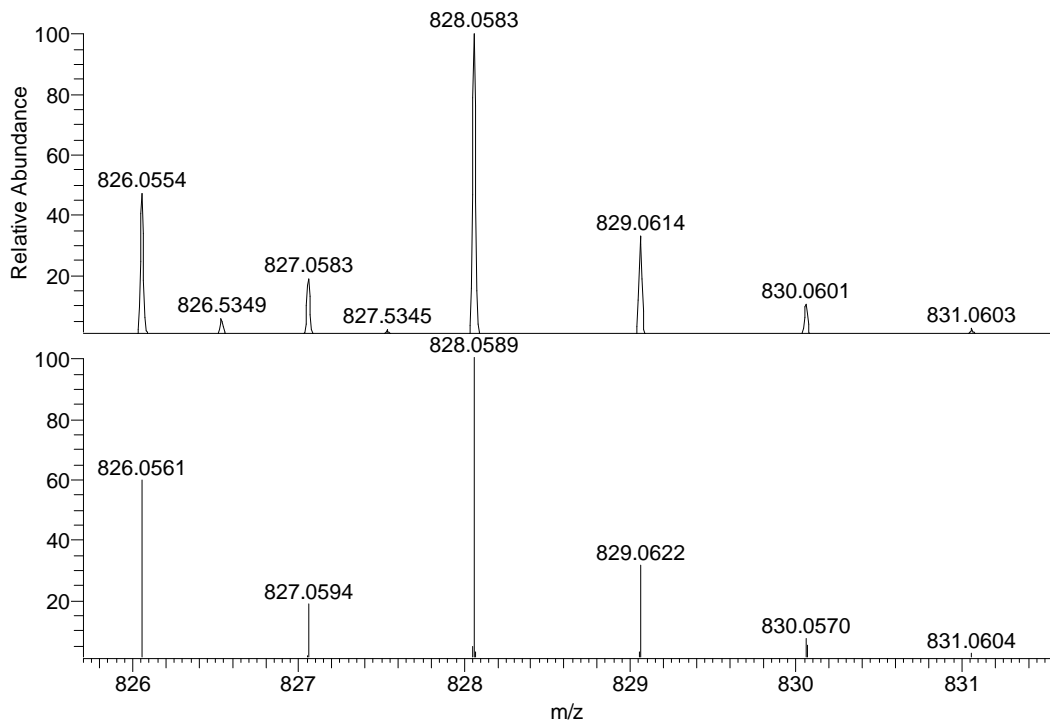


d)

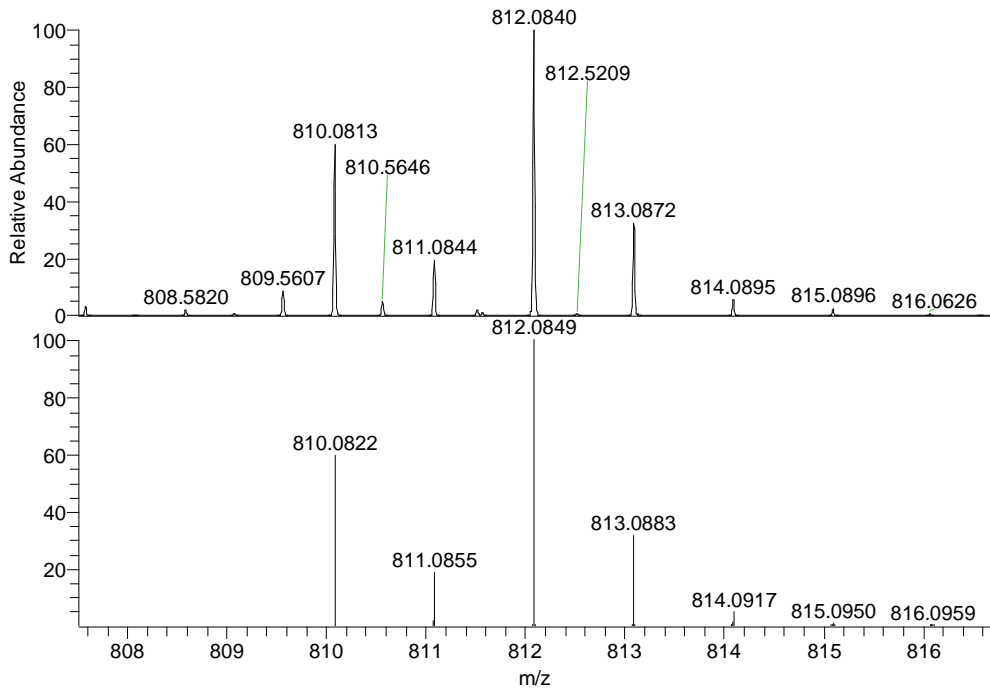


e)

**Figure S8** NMR analysis of **3** in DMSO- $d_6$ , a)  $^1\text{H}$ , b)  $^{13}\text{C}$ , c)  $^{19}\text{F}$  d)  $\{^1\text{H}, ^1\text{H}\}$  COSY and e)  $\{^{13}\text{C}, ^1\text{H}\}$  HSQC.

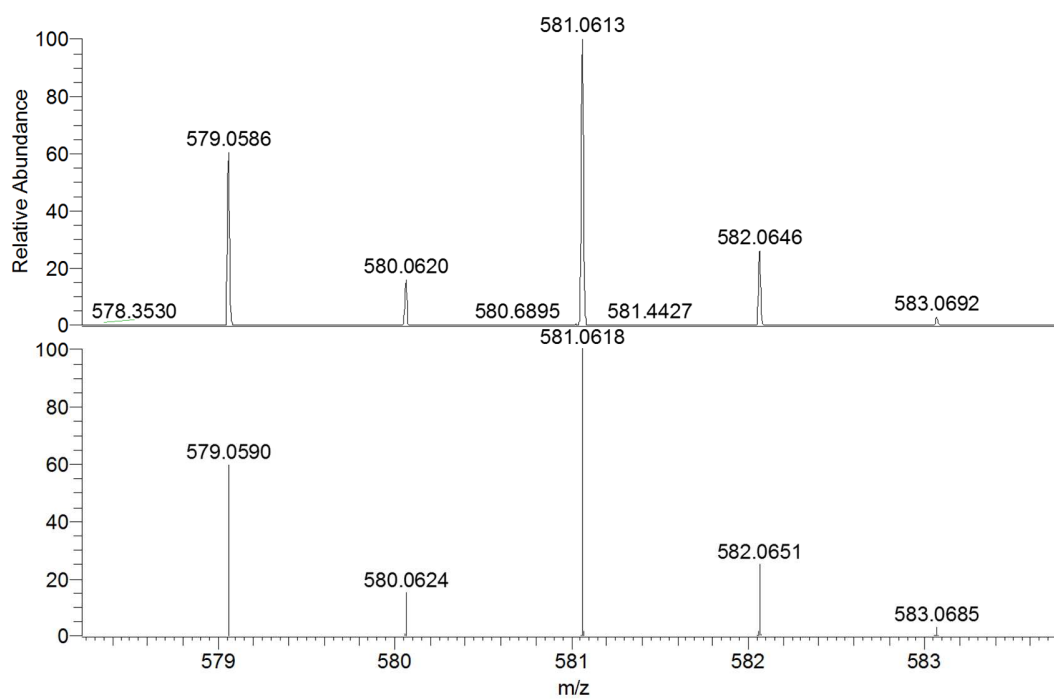


a)



b)

S15



c)

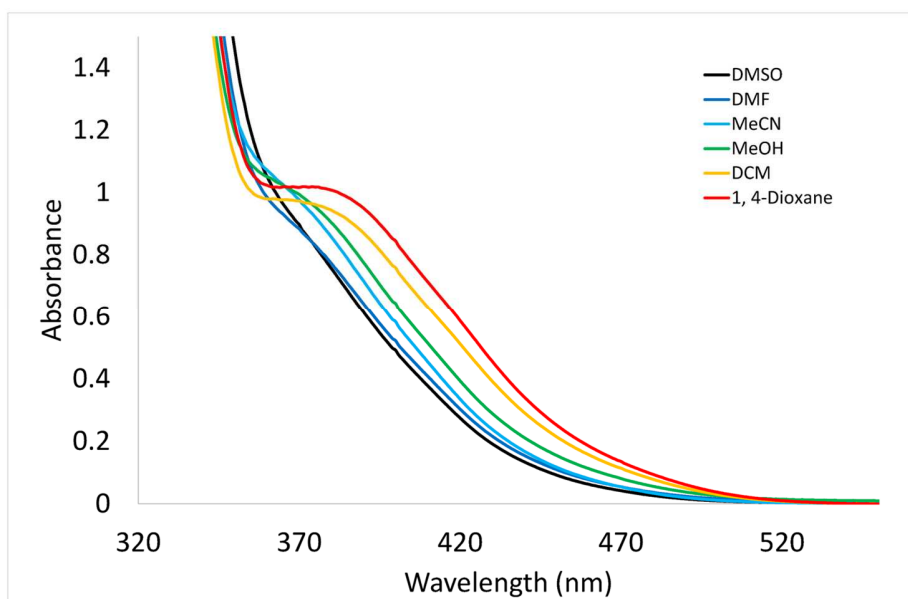
**Figure S9** Experimental (Up) and theoretical (down) ISOTOPIC pattern for the a)  $[M+K]^+$  (mass error: -0.6 ppm), b)  $[M+Na]^+$  (mass error: -0.9 ppm) and c)  $[M+H]^+$  ion (mass error: -0.5 ppm) of compound **3**.

### Single-crystal X-ray diffraction analysis

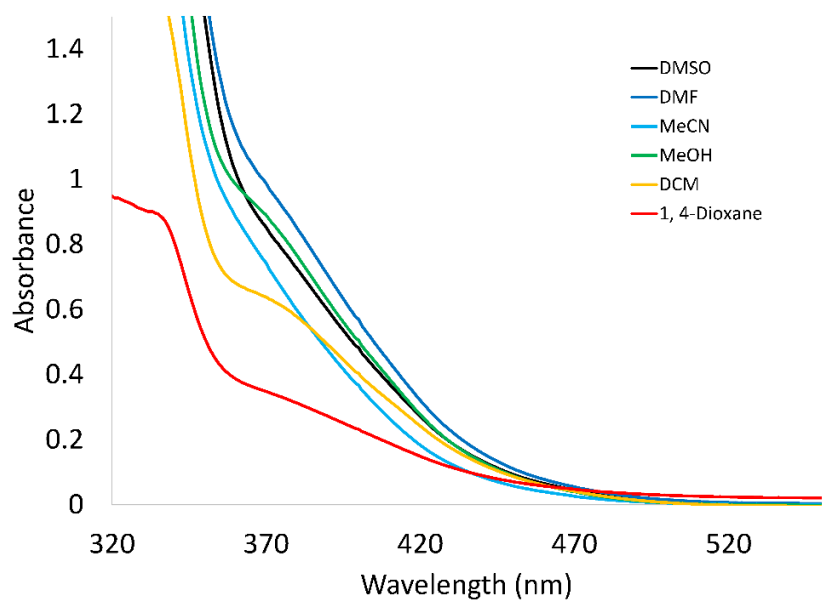
The crystal data of **3** were collected on a Bruker D<sub>8</sub> Quest diffractometer with a CMOS area detector and multi-layer mirror monochromatic MoK $\alpha$  radiation. The structure was solved using intrinsic phasing method,<sup>5</sup> refined with the SHELXT program,<sup>6</sup> and expanded using Fourier techniques. All non-hydrogen atoms were refined anisotropically. Hydrogen atoms were included in structure factors calculations. All hydrogen atoms were assigned to idealized geometric positions. To adapt C3\_v\_ symmetry the 1-2 and 1-3 distances in disordered solvent (CHCl\_3\_) were restrained to the same value in both residues. Atomic displacement parameters for all disordered atoms were restrained with similarity restraint SIMU, isotropic restrain ISOR and enhanced rigid bond restraint RIGU. Crystal data for **3**: C<sub>59</sub>H<sub>39</sub>Cl<sub>3</sub>F<sub>6</sub>N<sub>14</sub>O<sub>10</sub>Re<sub>2</sub>,  $M_r = 1696.79$ , orange plate, 0.395×0.166×0.032 mm<sup>3</sup>, Triclinic space group  $P\bar{1}$ ,  $a = 14.505(3)$  Å,  $b = 14.735(4)$  Å,  $c = 16.023(4)$  Å,  $\alpha = 70.934(19)^\circ$ ,  $\beta = 70.211(19)^\circ$ ,  $\gamma = 82.934(13)^\circ$ ,  $V = 3045.4(13)$  Å<sup>3</sup>,  $Z = 2$ ,  $\rho_{calcd} = 1.850$  g·cm<sup>-3</sup>,  $\mu = 4.193$  mm<sup>-1</sup>,  $F(000) = 1652$ ,  $T = 100(2)$  K,  $R_1 = 0.0258$ ,  $wR^2 = 0.0547$ , 13960 independent reflections [ $2\theta \leq 54.996^\circ$ ] and 886 parameters. Crystallographic data have been deposited with the Cambridge Crystallographic Data Centre as supplementary publication no. [CCDC. 2026701](https://www.ccdc.cam.ac.uk/data_request/cif) for compound **3**. These data can be obtained free of charge from The Cambridge Crystallographic Data Centre via [www.ccdc.cam.ac.uk/data\\_request/cif](https://www.ccdc.cam.ac.uk/data_request/cif).

**Table S1** Selected experimental bond lengths (Å) and angles (°) of **3**.

	<b>3</b>
Re1–N1_2	2.171(3)
Re1–C1_1	1.918(3)
Re1–C2_1	1.942(3)
Re1–C3_1	1.903(3)
Re1–N1_5	2.219(2)
Re1–N2_5	2.169(2)
C1_11–O1_1	1.149(4)
C2_11–O2_1	1.142(3)
C3_11–O3_1	1.155(3)
N1_2–Re1–N1_5	84.45(8)
N1_2–Re1–N12_5	88.29(8)
N1_2–Re1–C1_1	178.5(1)
N1_2–Re1–C2_1	88.6(1)
N1_2–Re1–C3_1	90.3(1)
C1_1–Re1–C2_1	89.9(1)
C2_1–Re1–C3_1	87.1(1)
C1_1–Re1–C3_1	89.6(1)
N1_5–Re1–C1_1	95.9(1)
N1_5–Re1–C2_1	104.0(1)
N12_5–Re1–C3_1	94.4(1)
N12_5–Re1–C1_1	93.2(1)
N12_5–Re1–C2_1	176.6(1)
N1_5–Re1–C3_1	167.6(1)
N1_5–Re1–N12_5	74.30(8)



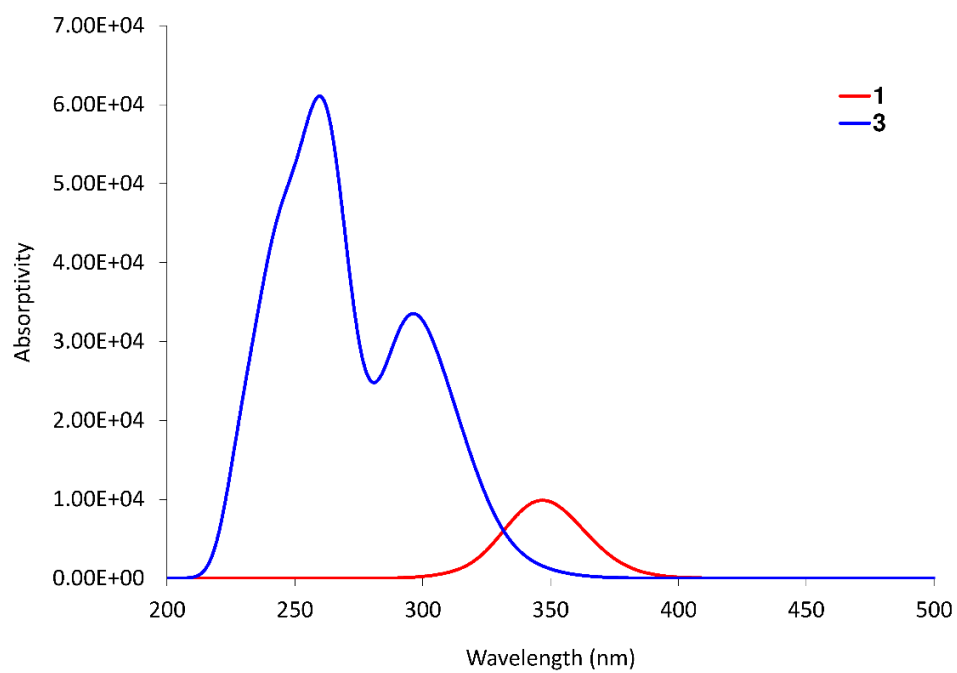
**Figure S10** Electronic absorption spectra of **3** in different solvents.



**Figure S11** Electronic absorption spectra of **1** in different solvents.

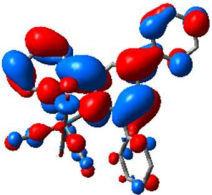
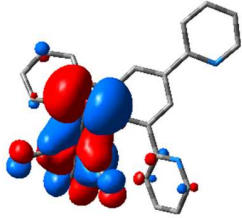
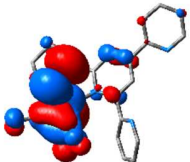
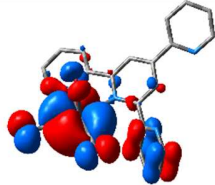
### Density functional theory (DFT) calculations

Ground-state geometry optimization and time dependent density functional (TDDFT) theory calculations were executed on modeling representing the molecular structures of **1**, and **3**. The starting geometry for the optimization of the triazolate complex is based on the crystallographic data of **3**. Becke 3-parameter (exchange) Lee–Yang–Parr (B3LYP) functional,<sup>7</sup> and the effective core potential (ECP) of the Hady and Wadt, LANL2DZ basis set,<sup>8</sup> were used to obtain the local minimum structures of the Re(I) complexes. Their energies were checked as minima on the potential energy surfaces by frequency calculations. TDDFT calculations were performed using CAM-B3LYP<sup>9</sup>/LANL2DZ method using the default polarizable continuum model (PCM) to introduce the effect of DMSO as a solvent. The first 30 singlet excited states were considered in the TDDFT calculations. All the calculations were done with Gaussian 03 package.<sup>10</sup> Visualization of the local minimum structures and Frontier molecular orbitals were carried out with the aid of Gauss view.<sup>11</sup>

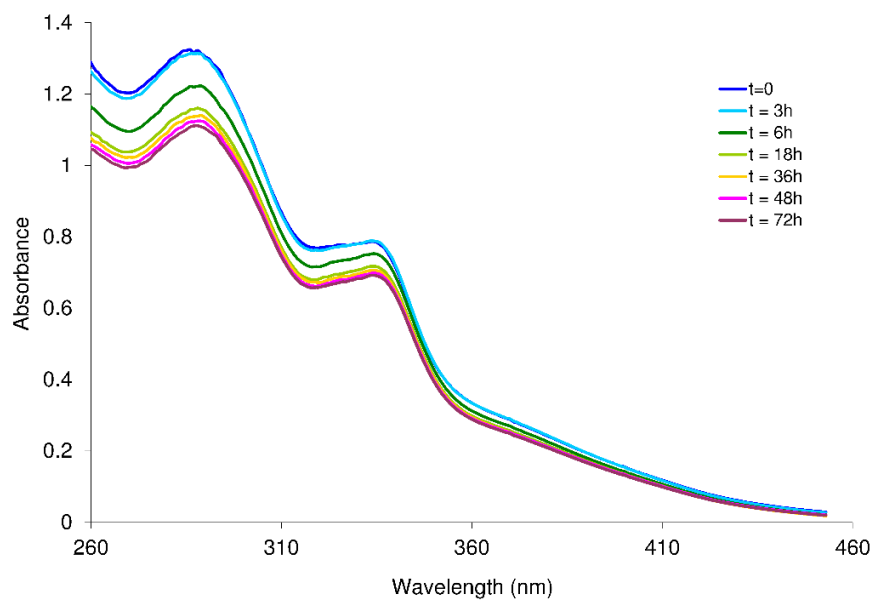


**Figure S12** Calculated electronic absorption spectra of **1** and **3**.

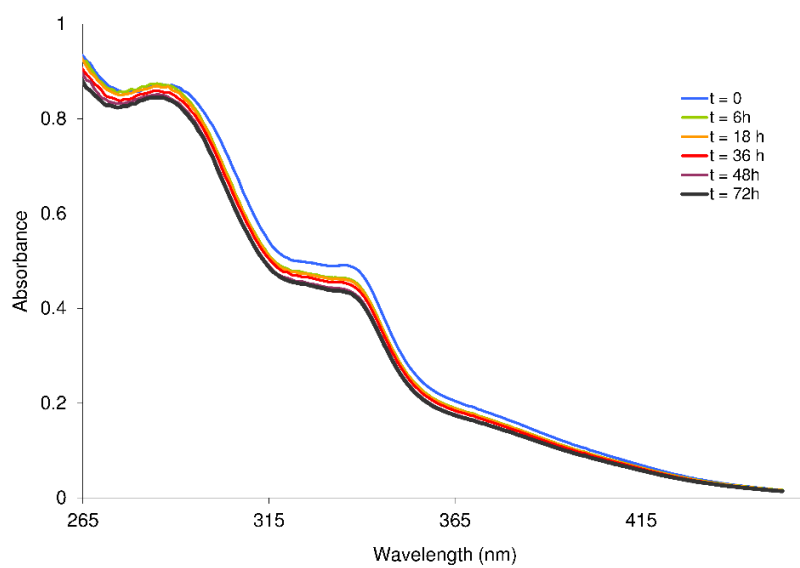
**Table S2** Selected FMO of **1** calculated at B3LYP/LANL2DZ level of theory.

Orbital	Molecular orbital plot	Orbital	Molecular orbital plot
LUMO		HOMO	
HOMO-1		HOMO-2	

<b>Table S3</b> Computed excitation energies (eV), electronic transition configurations and oscillator strengths ( $f$ ) of compounds <b>1</b> and <b>3</b> (selected, $f > 0.001$ ) (Selected)			
Energy (cm <sup>-1</sup> )	Wavelength (nm)	$f$	Major contributions
<b>• 1</b>			
28061	356	0.0105	HOMO→LUMO (90%)
28901	346	0.1267	HOMO-1→LUMO (92%)
31542	317	0.0078	HOMO-2→LUMO (78%)
<b>• 3</b>			
29654	337	0.0154	HOMO→LUMO (89%)
31906	313	0.1367	HOMO-1→LUMO (75%)
32672	306	0.0655	HOMO-2→LUMO (76%)
33915	294	0.2168	HOMO-3→LUMO (64%)
34202	292	0.1179	HOMO→LUMO+4 (29%)
37934	263	0.4246	HOMO-4→LUMO (32%)
40190	248	0.1371	HOMO-3→LUMO+1 (27%), HOMO-1→LUMO+1 (20%)
40719	245	0.1046	HOMO-2→LUMO+1 (32%)
40810	245	0.0747	HOMO→LUMO+2 (34%)



a)



b)

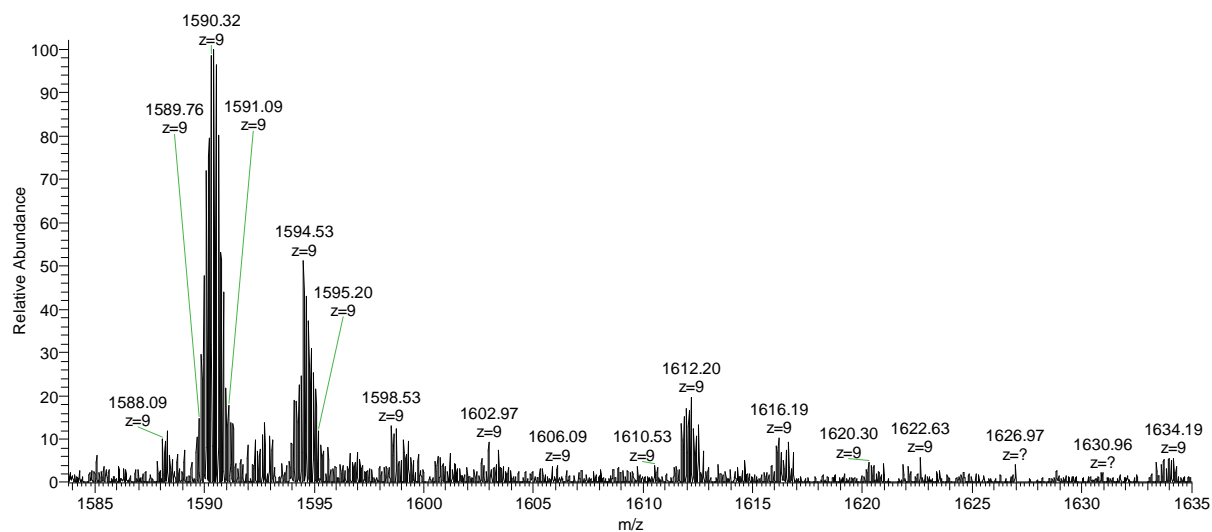
**Figure S13** UV-Vis spectra of a) **1** and b) **3** in 20% (v/v) DMSO/PBS (0.1 M) recorded as a function of time during the incubation for 72 h.

### **Cell viability**

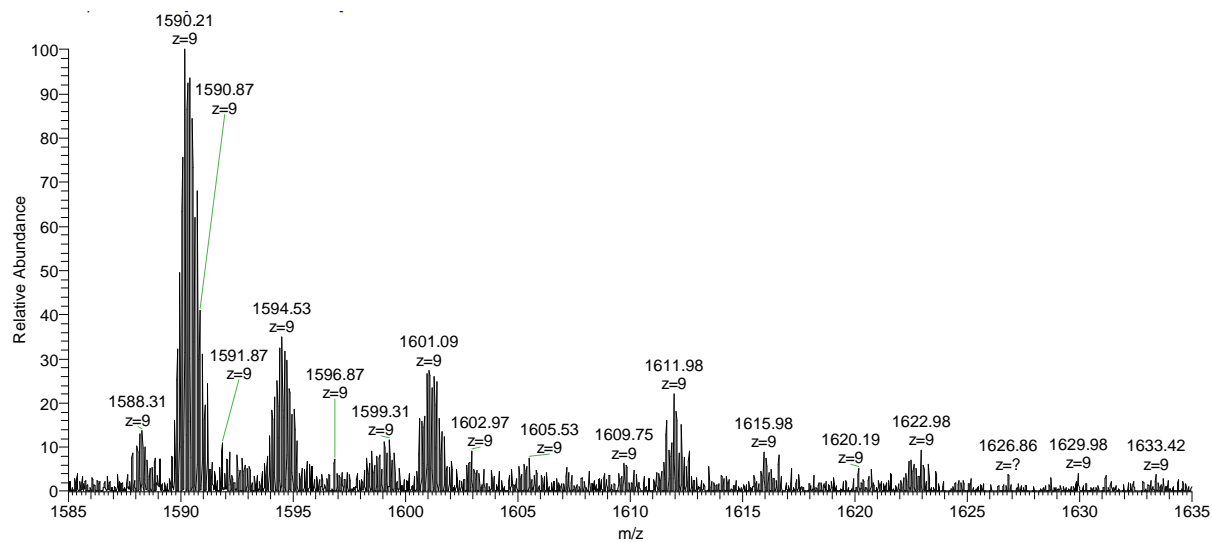
Human embryonic kidney HEK293 cells were counted manually in a Neubauer haemocytometer and then plated in the 384-well plates containing the terpyridine ligand to give a density of 5000 cells/well in a final volume of 50  $\mu$ L. Dulbecco's Modified Eagle Medium (DMEM) supplemented with 10% FBS was used as growth media and the cells were incubated together with the compounds for 20 h at 37  $^{\circ}$ C in 5% CO<sub>2</sub>. Cytotoxicity (or cell viability) was measured by Fluorescence (excitation 560/10, emission 590/10 nm) ( $F_{560/590}$ ), after addition of 5  $\mu$ L of 25  $\mu$ g/mL resazurin (2.3  $\mu$ g/mL final concentration) and after incubation for further 3 h at 37  $^{\circ}$ C in 5% CO<sub>2</sub>. The intensity was measured using Tecan M1000 Pro monochromator plate reader, using automatic gain calculation. CC<sub>50</sub> (the concentration at 50% cytotoxicity) was calculated by curve fitting the inhibition values vs. logC using a sigmoidal dose-response function, with variable fitting values for bottom, top and slope. The curve fitting was implemented using Pipeline Pilot's dose-response component, resulting in similar values to curve fitting tools such as GraphPad's Prism and IDBS's XIFit.

### **Lysozyme binding affinity**

Re(I) compounds were dissolved in DMSO and mixed with the aqueous solution of hen white egg lysozyme in 1:1, 1:10 and 1:20 reaction ratio to have a final solvent ratio of 20% (v/v) DMSO. The mixtures were subsequently injected into the mass spectrometer to record the positive mode ESI MS spectra. The MS spectra were recorded by direct introduction of the sample at a flow rate of 10  $\mu$ L min<sup>-1</sup>. The working conditions were as follows: spray voltage 3.80 KV, capillary voltage 45 V, and capillary temperature 320  $^{\circ}$ C. For acquisition, Thermo Xcalibur qual was used.

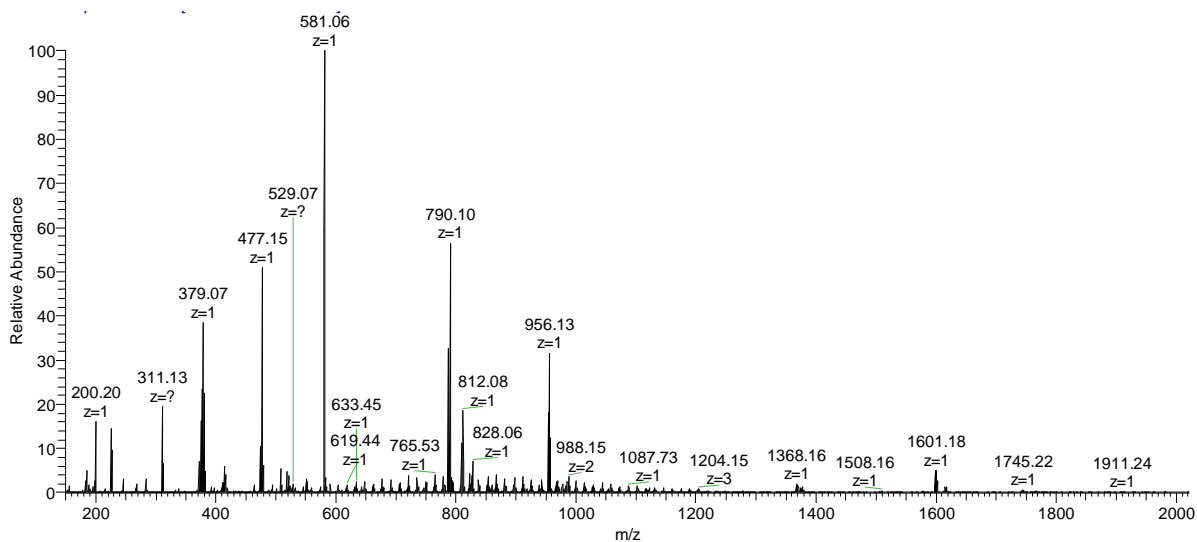


a)

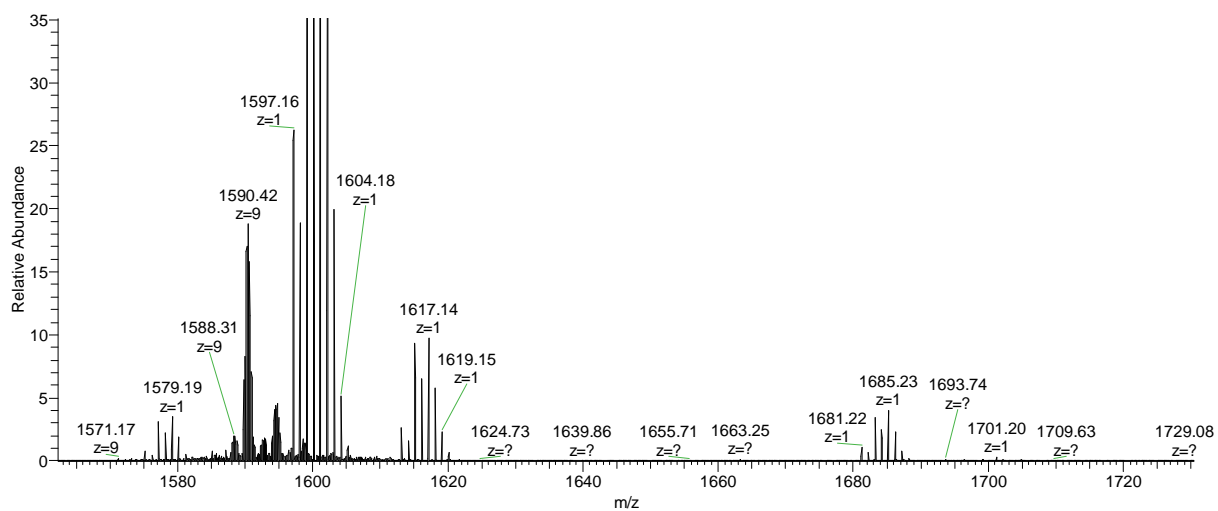


b)

**Figure S14** Deconvoluted ESI-MS spectra of HEWL treated with compound **1** in a) 1:10 and b) 1:20 (HEWL: complex).



a)



b)

**Figure S15 a)** ESI MS spectrum of **3**. **b)** Deconvoluted ESI-MS spectrum of HEWL treated with compound **3** in 1:20 (HEWL: complex).

## References

- 1 B.C. Hamper. Acetylenic esters from s-acylmethylenephosphoranes: Ethyl 4,4,4-trifluorotetrolate, *Org. Synth.*, 1992, **70**, 246.
- 2 A. Maroń, A. Szlapa, T. Klemens, S. Kula, B. Machura, S. Krompiec, J. Malecki, A. Świtlicka-Olszewska, K. Erfurt, and A. Chrobok, *Org. Biomol. Chem.*, 2016, **14**, 3793.
- 3 F. P. Gabbai, P. J. Chirik, D. E. Fogg, K. Meyer, D. J. Mindiola, L. L. Schafer, S. You, *Organometallics* 2016, **35**, 3255.
- 4 K. Peng, A. Friedrich and U. Schatzschneider, *Chem. Commun.*, 2019, **55**, 8142.
- 5 G. M. Sheldrick, *SHELXT, Acta Crystallogr.*, 2015, **A71**, 3.
- 6 G. M. Sheldrick. *Acta Crystallogr.*, 2008, **A64**, 112.
- 7 A.D. Becke, *J. Chem. Phys.*, 1993, **98**, 5648.
- 8 P.J. Hay and W.R. Wadt, *J. Chem. Phys.* 1985, **82**, 270; *J. Chem. Phys.* 1985, **82**, 284.
- 9 T. Yanai, D.P. Tew, and N.C. Handy, *Chem. Phys. Lett.* 2004, **393**, 51.
- 10 M. J. Frisch, G. W. Trucks, H. B. Schlegel, G. E. Scuseria, M. A. Robb, J. R. Cheeseman, V. G. Zakrzewski, J. A. Montgomery, R. E. Stratmann, J. C. Burant, S. Dapprich, J. M. Millam, A. D. Daniels, K. N. Kudin, M. C. Strain, O. Farkas, J. Tomasi, V. Barone, M. Cossi, R. Cammi, B. Mennucci, C. Pomelli, C. Adamo, S. Clifford, J. Ochterski, G. A. Petersson, P. Y. Ayala, Q. Cui, K. Morokuma, D. K. Malick, A. D. Rabuck, K. Raghavachari, J. B. Foresman, J. Cioslowski, J. V. Ortiz, A. G. Baboul, B. B. Stefanov, G. Liu, A. Liashenko, P. Piskorz, I. Komaromi, R. Gomperts, R. L. Martin, D. J. Fox, T. Keith, M.A. Al-Laham, C. Y. Peng, A. Nanayakkara, C. Gonzalez, M. Challacombe, P. M. W. Gill, B. G. Johnson, W. Chen, M.W. Wong, J.L. Andres, M. Head-Gordon, E.S. Replogle, J.A. Pople, GAUSSIAN 03 (Revision A.9), Gaussian, Inc., Pittsburgh, (2003).
- 11 A. Frisch, A. B. Nielson, A. J. Holder, Gaussview User Manual, Gaussian, Inc, Pittsburgh, PA 2000.